Cu2Ge(S3−xSex) Colloidal Nanocrystals: Synthesis, Characterization, and Composition-Dependent Band Gap Engineering

ARTICLE *in* JOURNAL OF THE AMERICAN CHEMICAL SOCIETY · APRIL 2013

Impact Factor: 12.11 · DOI: 10.1021/ja400452t · Source: PubMed

7 AUTHORS, INCLUDING:

Wen-Hua Zhang
Dalian Institute of Chemical Physics
40 PUBLICATIONS **1,395** CITATIONS
SEE PROFILE

Xin Xu
University of Science and Technology of China
111 PUBLICATIONS **1,107** CITATIONS
SEE PROFILE

JACS
JOURNAL OF THE AMERICAN CHEMICAL SOCIETY

Communication

pubs.acs.org/JACS

$Cu_2Ge(S_{3-x}Se_x)$ Colloidal Nanocrystals: Synthesis, Characterization, and Composition-Dependent Band Gap Engineering

Chi Yang,[†,‡] Bin Zhou,[†] Shu Miao,[†] Chunyan Yang,[†] Bing Cai,[†] Wen-Hua Zhang,*[,†] and Xin Xu*[,‡]

[†]State Key Laboratory of Catalysis, Dalian Institute of Chemical Physics, Chinese Academy of Sciences, and Dalian National Laboratory for Clean Energy, 457 Zhongshan Road, Dalian 116023, China

[‡]Department of Materials Science and Engineering, University of Science and Technology of China, Hefei 230026, China

Supporting Information

ABSTRACT: A facile solution-phase route was developed to synthesize a family of monodisperse $Cu_2Ge(S_{3-x}Se_x)$ alloyed nanocrystals (NCs) with controlled composition across the entire range ($0 \le x \le 3$). The band gaps of the resultant NCs can be engineered by tuning the compositions with a nearly linear relationship between them. The band structures of the NCs were studied by cyclic voltammetry and UV−vis absorption spectroscopy. The conducting behavior was revealed to be p-type for these NCs by photoelectrochemical measurements. Their photovoltaic applicability was finally assessed by fabricating solar cells with the $Cu_2Ge(S_2Se)$ NCs as light harvester and CdS nanorods as electron conducting materials.

Colloidal semiconductor nanocrystals (NCs) are of great interest due to their unique optical, magnetic, and electronic properties that are not achieved by their bulk counterparts. These NCs show advantages in low-cost synthesis and simple postprocessing, tunable properties, and high device performance. Colloidal semiconductor NCs have a wide range of applications in photovoltaics,[1] light-emitting diodes (LEDs),[2] bioimaging,[3] and so on. It has become increasingly facile to precisely control their size, shape, and crystal structure[4−6] for binary semiconductor NCs by colloidal synthesis, significantly promoting studies into their applications. Extension of colloidal synthesis to ternary and even quaternary semiconductor NCs may greatly expand this research platform. Moreover, the ability to tune the properties, especially band gap, to a target value is critical in achieving high-performance devices. However, this remains a big challenge for multicomponent semiconductor NCs. It is currently of great interest, but very limited successes have been reported in fabricating multicomponent NCs with properties that are consecutively tunable. To this end, growth of multicomponent NCs by alloying two constituents to produce desired alloyed NCs with tunable composition and properties has been described in several cases.[7−12] The alloyed NCs may not only inherit the properties of their parent materials but also exhibit new properties distinct from them.[7] Additionally, beside the size-dependent quantum confinement effect, the band gap energy of semiconductor NCs can be effectively tuned by varying their compositions via alloying of the constituents.

As environmentally friendly materials with the capability of band gap tailoring in a wide range, the Cu-based ternary and quaternary chalcogenides have received considerable interest in electronics. High-quality NCs of the Cu-based multicomponent NCs, including $Cu_2(Se,S)$,[12] $CuInS_2$,[13] $CuInSe_2$,[14] $Cu(In,Ga)(S,Se)_2$,[15] Cu_2SnSe_3,[16] Cu_2ZnSnS_4(CZTS),[17] $Cu_2ZnSnSe_4$(CZTSe),[18] $Cu_2CdSnSe_4$,[19] and $Cu_2ZnGeSe_4$,[20] have recently been prepared via colloidal synthesis. The band gap of the CZT-based chalcogenide NCs has been tuned by replacing the element S with Se to form alloyed CZT(S,Se) NCs with varying S/Se concentration in the final products.[21] Great application potentials have been demonstrated in photovoltaic cells[17,18,22] and thermoelectric devices[16b,19a,20,23] for these Cu-based multicomponent chalcogenide NCs.

Cu_2GeS_3 is a ternary semiconductor with a p-type direct band gap of 1.5 eV,[24] whereas Cu_2GeSe_3 has a p-type direct band gap of 0.78 eV.[25] Formation of the quaternary $Cu_2Ge(S_{3-x}Se_x)$ alloyed NCs could thereby tune the band gaps to the ideal range for solar light absorption. Cabot et al.[26] most recently exploited the colloidal synthesis of Cu_2GeSe_3 nanoparticles and their thermoelectric properties. However, it remains a challenge to control the fabrication of monodisperse $Cu_2Ge(S_{3-x}Se_x)$ NCs with tunable S/Se compositions by colloidal chemistry. To achieve the $Cu_2Ge(S_{3-x}Se_x)$ alloyed NCs, the growth kinetics of the two constituent materials must be sufficiently close and the reaction conditions highly compatible. However, the S precursor and the Se precursor in colloidal synthesis usually show different reactivity, which hampers the formation of the desired alloy. Herein, we report a facile solution approach to the $Cu_2Ge(S_{3-x}Se_x)$ alloyed NCs in which the contents of S and Se can be varied across the entire compositional range ($0 \le x \le 3$). The resultant NCs exhibits band gaps ranging from 2.16 to 1.20 eV with varying S/Se ratios in the products. Their microstructures were studied by X-ray diffraction (XRD), transmission electron microscopy (TEM), and high-resolution (HR) TEM, and the band structures were estimated by a combination of cyclic voltammetry (CV) and UV−visisible−near-infrared (UV-vis-NIR) absorption spectroscopy. We have also assessed their applicability as photovoltaic materials by fabricating solar cells consisting of n-type CdS nanorods and p-type $Cu_2Ge(S_2Se)$ NCs.

The synthesis of $Cu_2Ge(S_{3-x}Se_x)$ colloidal NCs was carried out in oleylamine (OLA) solution by a hot-injection method. In a typical synthesis, copper(II) acetylacetonate [$Cu(acac)_2$] was dissolved in OLA in an inert atmosphere. The flask loaded with $Cu(acac)_2$/OLA solution was then heated to 125 °C under

Received: January 21, 2013
Published: April 6, 2013

dx.doi.org/10.1021/ja400452t | J. Am. Chem. Soc. 2013, 135, 5958−5961

vacuum, and then germanium tetrachloride ($GeCl_4$) was injected. Meanwhile, elemental S and Se with specific molar ratios were dissolved in OLA, also under inert conditions, and then injected into the OLA solution containing $Cu(acac)_2$ and $GeCl_4$ at 160 °C. The mixed solution was finally heated to 280 °C and maintained for 2 h to yield $Cu_2Ge(S_{3-x}Se_x)$ NCs.

Figure 1 shows the powder XRD patterns of the $Cu_2Ge(S_{3-x}Se_x)$ NCs. The major diffraction peaks gradually shift

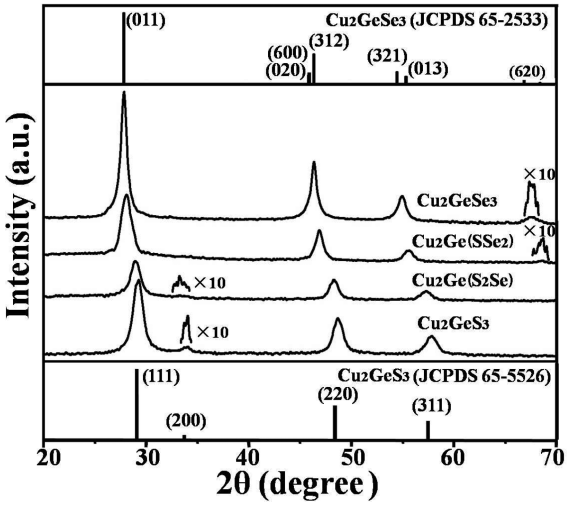

Figure 1. XRD patterns for the $Cu_2Ge(S_{3-x}Se_x)$ NCs with various S/Se ratios.

toward lower angles with increasing Se contents, and no peak-splitting appears. This indicates gradually enlarged lattice constants arising from substitution of the significantly larger Se^{2-} to the smaller S^{2-} in the lattices and rules out phase separation or separated nucleation of Cu_2GeS_3 and Cu_2GeSe_3 during the growth of the $Cu_2Ge(S_{3-x}Se_x)$ NCs. This is in line with the behavior of homogeneous alloy characterized by Vegard's law,[27] confirming the formation of alloyed NCs with homogeneous distribution of S and Se in the $Cu_2Ge(S_{3-x}Se_x)$ matrix. Close investigation into the XRD patterns reveals that the three major reflections along with the weak diffraction peak (at $2\theta \approx 33.7°$) for the Cu_2GeS_3 and $Cu_2Ge(S_2Se)$ NCs can be indexed respectively as the (110), (220), (311), and (200) planes, matching perfectly with a cubic structure of Cu_2GeS_3. In contrast, for the $Cu_2Ge(SSe_2)$ and Cu_2GeSe_3 NCs, the major diffraction peak at $2\theta \approx 27°$ and a weak one at $2\theta \approx 68.3°$ could be indexed respectively as (011) and (004) reflections of the orthorhombic phase of Cu_2GeSe_3. The broadened peaks at $2\theta \approx 46°$ can be attributed to the overlap of (020), (600), and (312) reflections and the peak at $2\theta \approx 55°$ to the overlap of the (321) and (013) reflections of the orthorhombic Cu_2GeSe_3. Therefore, the as-prepared $Cu_2Ge(SSe_2)$ and Cu_2GeSe_3 NCs exhibit orthorhombic structure.

TEM was performed to further investigate the microstructures of the $Cu_2Ge(S_{3-x}Se_x)$ ($0 \le x \le 3$) NCs. TEM images for the Cu_2GeS_3 NCs are presented in Figure 2, and images for other NCs are shown in the Supporting Information. The low-magnification TEM images show that as-prepared $Cu_2Ge(S_{3-x}Se_x)$ ($0 \le x \le 3$) NCs have narrow size distributions with a relative standard deviation of 5−10%, and that the average sizes of the NCs are enlarged upon increasing the Se content to a certain degree (Figure S4). As shown in Table 1, the smallest particle size was found for Cu_2GeS_3 NCs with a mean size of ~11

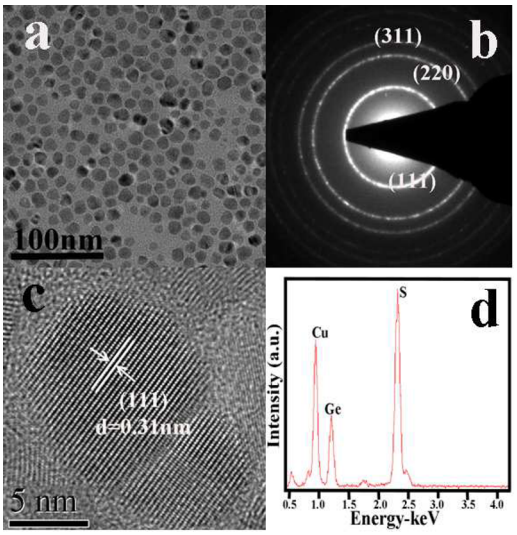

Figure 2. (a) Low-magnification TEM images, (b) SAED patterns, (c) HRTEM images, and (d) EDX spectrum for the Cu_2GeS_3 NCs.

nm and the largest for Cu_2GeSe_3 with a mean size of ~19 nm. A number of NCs show multiple contrasts in Figure 2a. This is probably associated with two factors: (a) crystallographic changes in the lattice, e.g., grain boundaries and twinning, which make the particle actually polycrystalline and produce distinct contrast changes within the particle, and (b) slight distortion of the local lattice caused by defects within a single crystal, which shows gradual contrast change under an electron beam. Figure 2b presents the polycrystalline selected area electron diffraction (SAED) patterns of Cu_2GeS_3 NCs, showing clearly three diffraction rings that match well with the (111), (220), and (311) lattice planes of the cubic Cu_2GeS_3, which is in line with the XRD results. HRTEM images of the $Cu_2Ge(S_{3-x}Se_x)$ ($0 \le x \le 3$) NCs show clearly the lattice fringes for all NCs, clearly indicating that they are well crystalline. Specifically, HRTEM images for the Cu_2GeS_3 NCs in Figure 2c show *d*-spacing of 0.31 nm, indexed as the (111) plane of cubic Cu_2GeS_3. These results further demonstrate that the as-prepared Cu_2GeS_3 NCs exhibit cubic structure. Similarly, the as-synthesized $Cu_2Ge(S_2Se)$ can also be attributed to cubic structure, while $Cu_2Ge(SSe_2)$ and Cu_2GeSe_3 NCs can be assigned to the orthorhombic phase. The chemical compositions of the $Cu_2Ge(S_{3-x}Se_x)$ NCs revealed by energy-dispersive X-ray spectroscopy (EDX) are displayed in Table 1. Increase in the ratios of Se/S in the precursors results in an increase of the Se contents in the final products, and the atomic ratios of Cu/Ge/S/Se in the products are in close agreement with the nominal compositions of $Cu_2Ge(S_{3-x}Se_x)$ ($0 \le x \le 3$), demonstrating successful formation of the alloyed $Cu_2Ge(S_{3-x}Se_x)$ NCs with the variation of S/Se in the entire compositional range ($0 \le x \le 3$).

The UV-vis-NIR absorption spectra of the $Cu_2Ge(S_{3-x}Se_x)$ NCs were measured to study their optical properties. The band gap energies (E_g) were calculated by plotting the square of the absorption coefficiency (α) as a function of photon energy ($h\nu$) and extrapolating the linear portion to intercept the x abscissa (Figure S5). It is found that increasing the Se contents in the $Cu_2Ge(S_{3-x}Se_x)$ ($0 \le x \le 3$) matrix results in a monotonous decrease of the band gap energies, i.e., a nearly linear relationship between the band gaps and the Se contents in the NCs. This is consistent with Vegard's law, again demonstrating formation of

dx.doi.org/10.1021/ja400452t | J. Am. Chem. Soc. 2013, 135, 5958−5961

Table 1. Compositional Analysis of $Cu_2Ge(S_{3-x}Se_x)$ Nanocrystals Prepared Herein[a]

$Cu_2Ge(S_{3-x}Se_x)$	Cu/Ge/S/Se molar ratio in precursor	Cu/Ge/S/Se molar ratio in products	E_g (eV)	CBM (eV)	mean particle size (nm)
Cu_2GeS_3 ($x = 0$)	2.0:2.0:4.0:0.0	2.0:1.0:3.1:0.0	2.16 ± 0.04	−3.88 ± 0.01	10.8
$Cu_2Ge(S_2Se)$ ($x = 1$)	2.0:2.0:2.0:1.0	2.0:1.2:2.0:1.2	1.84 ± 0.03	−3.93 ± 0.01	11.3
$Cu_2Ge(SSe_2)$ ($x = 2$)	2.0:2.0:1.0:2.0	2.0:1.1:1.1:2.2	1.61 ± 0.01	−3.94 ± 0.01	15.4
Cu_2GeSe_3 ($x = 3$)	2.0:2.0:0.0:4.0	2.0:1.1:0.0:3.3	1.20 ± 0.02	−3.97 ± 0.01	19.2

[a]The final compositions were analyzed by EDX.

the homogeneous alloyed $Cu_2Ge(S_{3-x}S_x)$ ($0 \le x \le 3$) in the present experiments.[27]

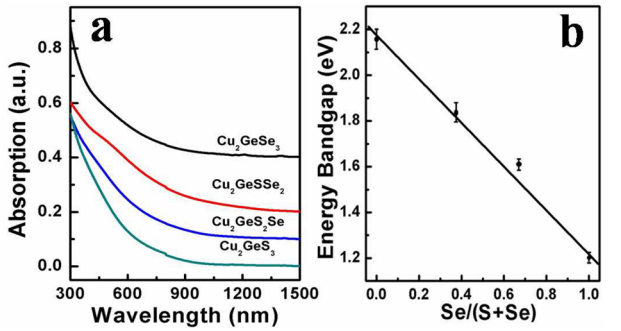

Figure 3. (a) UV-vis-NIR absorption spectra for the $Cu_2Ge(S_{3-x}Se_x)$ NCs with various S/Se ratios. (b) Relationship between the band gaps of the NCs and the content of Se in the products.

It is of critical importance to understand the band energy levels of a material prior to exploiting its application in electronics such as photovoltaic cells, and CV has been demonstrated to be an effective tool in this issue. The conduction band minimum (CBM) of a semiconductor can be calculated from the onset reduction potential (E_{red}) according to the equation $E_{CBM} = -(E_{red} + 4.71)$ eV, where Ag/Ag^+ electrode is employed as the reference.[28] A typical CV curve for a Cu_2GeS_3 NCs thin film, deposited on a glassy carbon working electrode, is presented in Figure 4a. E_{red} appears at −0.83 V relative to the Ag/Ag^+

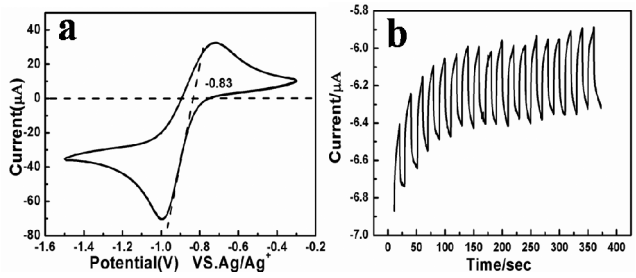

Figure 4. (a) Cyclic voltammogram and (b) transient photocurrent response of the Cu_2GeS_3 NCs film.

reference electrode. The CBM of the Cu_2GeS_3 NCs was thereby determined to be −3.88 eV from the vacuum level, and the valence band maximum (VBM) was then estimated to be −6.04 eV according to the 2.16 eV optical band gap. The band energy levels for all other $Cu_2Ge(S_{3-x}Se_x)$ NCs could also be estimated by the same procedure, and the results are summarized in Table 1. It is found that the CBMs of the $Cu_2Ge(S_{3-x}Se_x)$ NCs decreased slightly with increasing Se content in the products. Moreover, photoelectrochemical properties of as-synthesized $Cu_2Ge(S_{3-x}Se_x)$ ($0 \le x \le 3$) NCs were evaluated by measuring the transient photocurrents of the NCs film on ITO in a photoelectrochemical cell. Photocurrent generated from the NC electrodes was negative (Figure 4b), which is typical of p-type semiconductor behavior. Therefore, to assess the potential for their application in solar energy, it is suitable to employ the p-type $Cu_2Ge(S_{3-x}Se_x)$ NCs and n-type CdS to form photovoltaic devices.

Finally, due to the ease and cost-effectiveness in processing NC solar cells, photovoltaic cells consisting of semiconductor NCs fabricated by full solution approach have recently drawn much attention.[1,29] The solar cell devices were hence fabricated in the configuration of FTO/CdS NRs/$Cu_2Ge(S_2Se)$ NCs/MoO_3/Au to assess the photovoltaic potentials of $Cu_2Ge(S_{3-x}Se_x)$ NCs by a full solution approach. $Cu_2Ge(S_2Se)$ was chosen as model material to study photovoltaic properties of the NCs prepared herein because its band energy levels are compatible to those of CdS and because of its ease in forming smooth films by solution approach. The CdS nanorods on FTO substrates were prepared by hydrothermal growth,[30] and then $Cu_2Ge(S_2Se)$ NCs were deposited onto them by spin coating of a NCs solution via a layer-by-layer approach. A MoO_3 interfacial layer was then deposited via thermal evaporation since it favors hole injection and extraction and eases the formation of ohmic contact for the back electrode, resulting in relatively high device performance for solar cells.[31] Figure 5 compares the typical

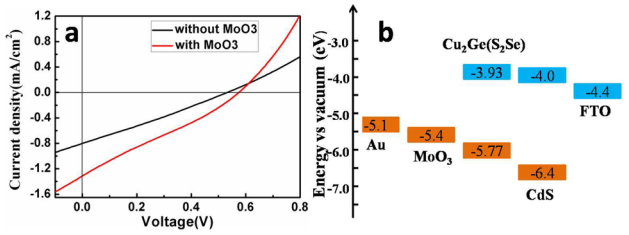

Figure 5. (a) Photovoltaic characteristics of the $Cu_2Ge(S_2Se)$NCs/CdS NR array solar cells with and without MoO_3 interfacial layers. (b) Scheme of the energy levels of the materials employed in the devices.

photovoltaic characteristics of the $Cu_2Ge(S_2Se)$ NCs with and without MoO_3 interfacial layers. The device without MoO_3 shows an open-circuit voltage (V_{oc}) of 0.53 V, short-circuit current density (J_{sc}) of 0.80 mA/cm^2, and fill factor (FF) of 0.28, yielding a power conversion efficiency (η) of 0.12% under AM1.5G illumination. In contrast, the PV device with MoO_3 buffer layer shows enhanced V_{oc} = 0.57 V and J_{sc} = 1.31 mA/cm^2, while FF is kept basically unchanged, resulting in 0.20% efficiency. The device efficiency is still low primarily due to the low J_{sc} and FF, which arise from large series resistance and small shunt resistance. The large series resistance may come from the very abundant grain boundaries between NCs that were not processed at high temperatures after deposition. These results

dx.doi.org/10.1021/ja400452t | J. Am. Chem. Soc. 2013, 135, 5958−5961

indicate the application potentials of the $Cu_2Ge(S_{3-x}Se_x)$ NCs in solar cells if the cell fabrication can be optimized.

In summary, we have introduced a facile solution synthesis of $Cu_2Ge(S_{3-x}Se_x)$ colloidal nanocrystals across the entire compositional range ($0 \leq x \leq 3$). The band gaps of the NCs can be effectively tailored by tuning their compositions, and the dependence of the band gaps on alloy compositions is found to be almost linear. The band structures of the NCs were studied by a combination of cyclic voltammetry and UV−vis absorption spectroscopy. Initial photovoltaic devices consisting of $Cu_2Ge(S_2Se)$ NCs as light absorber showed efficiency of 0.20% under AM1.5 illumination. These results should be favorable for improving our understanding of their basic properties and their device applicability.

■ ASSOCIATED CONTENT

Supporting Information

Experimental details, TEM, HRTEM, SEAD, EDX, size distributions of NCs, band gap determination from the UV−vis absorption spectra, CV, cross-section SEM images, and the dark I-V curve of the solar cell. This material is available free of charge via the Internet at http://pubs.acs.org.

■ AUTHOR INFORMATION

Corresponding Author

whzhang@dicp.ac.cn; xuxin@ustc.edu.cn

Notes

The authors declare no competing financial interest.

■ ACKNOWLEDGMENTS

We are very thankful to Prof. Daocheng Pan and Dr. Gang Wang for fruitful disccusions on the PV device fabrication. This work is financially supported from NSFC (No. 20873141), the "Hundred Talents Program", the Solar Energy Initiative of the Knowledge Innovation Program of the Chinese Academy of Sciences (Grant. No. KGCX2-YW-395), and the National Basic Research Program of China (No. 2012CB922004).

■ REFERENCES

(1) (a) Huynh, W. U.; Dittmer, J. J.; Alivisatos, A. P. *Science* **2002**, *295*, 2425. (b) Pattantyus-Abraham, A. G.; Kramer, I. J.; Wang, X. H.; Konstantatos, G.; Debnath, R.; Levina, L.; Raabe, I.; Nazeeruddin, M. K.; Gratzel, M.; Sargent, E. H. *ACS Nano* **2010**, *4*, 3374.

(2) (a) Bowers, M. J.; McBride, J. R.; Rosenthal, S. J. *J. Am. Chem. Soc.* **2005**, *127*, 15378. (b) Dang, C.; Lee, J.; Zhang, Y.; Han, J.; Breen, C.; Steckel, J. S.; Coe-Sullivan, S.; Nurmikko, A. *Adv. Mater.* **2012**, *24*, 5915.

(3) Kim, J.; Piao, Y.; Hyeon, T. *Chem. Soc. Rev.* **2009**, *38*, 372.

(4) (a) Kwon, S.; Hyeon, T. *Acc. Chem. Res.* **2008**, *41*, 1696. (b) Yu, W. W.; Qu, L. H.; Guo, W. Z.; Peng, X. G. *Chem. Mater.* **2003**, *15*, 2854.

(5) (a) Peng, X. G.; Manna, L.; Yang, W. D.; Wickham, J.; Scher, E.; Kadavanich, A.; Alivisatos, A. P. *Nature* **2000**, *404*, 59. (b) Son, J. S.; Wen, X.-D.; Joo, J.; Chae, J.; Baek, S.-il; Park, K.; Kim, J. H.; An, K. J.; Yu, J. H.; Kwon, S. G.; Choi, S.-H.; Wang, Z.; Kim, Y.-W.; Kuk, Y.; Hoffmann, R.; Hyeon, T. *Angew. Chem., Int. Ed.* **2009**, *48*, 6861. (c) Liu, S.; Guo, X.; Li, M.; Zhang, W.-H.; Liu, X.; Li, C. *Angew. Chem., Int. Ed.* **2011**, *50*, 12050. (d) Jeong, S.; Yoo, D.; Jang, J.-t.; Kim, M.; Cheon, J. *J. Am. Chem. Soc.* **2012**, *134*, 18233.

(6) (a) Wang, D.; Li, Y. *Adv. Mater.* **2011**, *23*, 1044. (b) Lu, X.; Zhuang, Z.; Peng, Q.; Li, Y. *Chem. Commun.* **2011**, *47*, 3141. (c) Sahu, V.; Qi, L.; Kang, M. S.; Deng, D.; Norris, J. *J. Am. Chem. Soc.* **2011**, *133*, 6509.

(7) Regulacio, M. D.; Han, M.-Y. *Acc. Chem. Res.* **2010**, *43*, 621.

(8) (a) Swafford, L. A.; Weigand, L. A.; Bowers, M. J.; McBride, J. R.; Rapaport, J. L.; Watt, T. L.; Dixit, S. K.; Feldman, L. C.; Rosenthal, S. J. *J. Am. Chem. Soc.* **2006**, *128*, 12299. (b) Lovingood, D. D.; Oyler, R. E.; Strouse, G. F. *J. Am. Chem. Soc.* **2008**, *130*, 17004.

(9) Zhong, X.; Feng, Y.; Knoll, W.; Han, M. *J. Am. Chem. Soc.* **2003**, *125*, 13559.

(10) Sung, Y.-M.; Lee, Y.-J.; Park, K.-S. *J. Am. Chem. Soc.* **2006**, *128*, 9002.

(11) Deng, Z.; Yan, H.; Liu, Y. *J. Am. Chem. Soc.* **2009**, *131*, 17744.

(12) Wang, J.-J.; Xue, D.-J.; Guo, Y.-G.; Hu, J.-S.; Wan, L.-J. *J. Am. Chem. Soc.* **2011**, *133*, 18558.

(13) (a) Kruszynska, M.; Borchert, H.; Parisi, J.; Kolny-Olesiak, J. *J. Am. Chem. Soc.* **2010**, *132*, 15976. (b) Norako, M. E.; Franzman, M. A.; Brutchey, R. L. *Chem. Mater.* **2009**, *21*, 4299.

(14) (a) Norako, M. E.; Brutchey, R. L. *Chem. Mater.* **2010**, *22*, 1613. (b) Koo, B.; Patel, R. N.; Korgel, B. A. *J. Am. Chem. Soc.* **2009**, *131*, 3134. (c) Guo, Q.; Kim, S. J.; Kar, M.; Shafarman, W. N.; Birkmire, R. W.; Stach, E. A.; Agrawal, R.; Hillhouse, H. W. *Nano Lett.* **2008**, *8*, 2982.

(15) (a) Wang, Y.-H. A.; Zhang, X.; Bao, N.; Lin, B.; Gupta, A. *J. Am. Chem. Soc.* **2011**, *133*, 11072. (b) Guo, Q.; Ford, G. M.; Hillhouse, H. W.; Agrawal, R. *Nano Lett.* **2009**, *9*, 3060. (c) Panthani, M. G.; Akhavan, V.; Goodfellow, B.; Schmidtke, J. P.; Dunn, L.; Dodabalapur, A.; Barbara, P. F.; Korgel, B. A. *J. Am. Chem. Soc.* **2008**, *130*, 16770.

(16) (a) Norako, M. E.; Greaney, M. J.; Brutchey, R. L. *J. Am. Chem. Soc.* **2012**, *134*, 23. (b) Ibáñez, M.; Cadavid, D.; Anselmi-Tamburini, U.; Zamani, R.; Gorsse, S.; Li, W.; López, A. M.; Morante, J. R.; Arbiol, J.; Cabot, A. *J. Mater. Chem. A* **2013**, *1*, 1421.

(17) (a) Riha, S. C.; Parkinson, B. A.; Prieto, A. L. *J. Am. Chem. Soc.* **2009**, *131*, 12054. (b) Steinhagen, C.; Panthani, M. G.; Akhavan, V.; Goodfellow, B.; Koo, B.; Korgel, B. A. *J. Am. Chem. Soc.* **2009**, *131*, 12554. (c) Guo, Q.; Hillhouse, H. W.; Agrawal, R. *J. Am. Chem. Soc.* **2009**, *131*, 11672. (d) Singh, A.; Geaney, H.; Laffir, F.; Ryan, K. M. *J. Am. Chem. Soc.* **2012**, *134*, 2910.

(18) Shavel, A.; Arbiol, J.; Cabot, A. *J. Am. Chem. Soc.* **2010**, *132*, 4514.

(19) (a) Fan, F.-J.; Yu, B.; Wang, Y.-X.; Zhu, Y.-L.; Liu, X.-J.; Yu, S.-H.; Ren, Z. *J. Am. Chem. Soc.* **2011**, *133*, 15910. (b) Ibáñez, M.; Zamani, R.; Li, M.; Shavel, A.; Arbiol, J.; Morante, J. M.; Cabot, A. *Cryst. Growth Des.* **2012**, *12*, 1085.

(20) Ibáñez, M.; Zamani, R.; LaLonde, A.; Cadavid, D.; Li, W.; Shavel, A.; Arbiol, J.; Morante, J. R.; Gorsse, S.; Snyder, G. J.; Cabot, A. *J. Am. Chem. Soc.* **2012**, *134*, 4060.

(21) Riha, S. C.; Parkinson, B. A.; L. Prieto, A. *J. Am. Chem. Soc.* **2011**, *133*, 15272.

(22) (a) Guo, Q.; Ford, G. M.; Yang, W.-C.; Walker, B. C.; Stach, E. A.; Hillhouse, H. W.; Agrawal, R. *J. Am. Chem. Soc.* **2010**, *132*, 17384. (b) Ford, G. M.; Guo, Q.; Agrawal, R.; Hillhouse, H. W. *Chem. Mater.* **2011**, *23*, 2626.

(23) Yang, H.; Jauregui, L. A.; Zhang, G.; Chen, Y. P.; Wu, Y. *Nano Lett.* **2012**, *12*, 540.

(24) Tsuji, I.; Shimodaira, Y.; Kato, H.; Kobayashi, H.; Kudo, A, *Chem. Mater.* **2010**, *22*, 1402.

(25) Marcano, G.; Nieves, L. *J. Appl. Phys.* **2000**, *87*, 1284.

(26) Ibáñez, M.; Zamani, R.; Li, W.; Cadavid, D.; Gorsse, S.; Katcho, N. A.; Shavel, A.; López, A. M.; Morante, J. R.; Arbiol, J.; Cabot, A. *Chem. Mater.* **2012**, *24*, 4615.

(27) Vegard, L.; Schjelderup, H. *Phys. Z.* **1917**, *18*, 93.

(28) Zhong, H.; Lo, S. S.; Mirkovic, T.; Li, Y.; Ding, Y.; Li, Y.; Scholes, G. D. *ACS Nano* **2010**, *4*, 5253.

(29) (a) Tang, J.; Sargent, E. H. *Adv. Mater.* **2011**, *23*, 12. (b) Tang, J.; Kemp, K. W.; Hoogland, S.; Jeong, K. S.; Liu, H.; Levina, L.; Furukawa, M.; Wang, X.; Debnath, R.; Cha, D.; Chou, K. W.; Fischer, A.; Amassian, A.; Asbury, J. B.; Sargent, E. H. *Nat. Mater.* **2011**, *10*, 765.

(30) Yang, C.; Liu, S.; Li, M.; Wang, X.; Zhu, J.; Chong, R.; Yang, D.; Zhang, W.-H.; Li, C. *J. Colloid Interface Sci.* **2013**, *393*, 58.

(31) (a) Meyer, J.; Hamwi, S.; Kröger, M.; Kowalsky, W.; Riedl, T.; Kahn, A. *Adv. Mater.* **2012**, *24*, 5408. (b) Brown, P. R.; Lun, R. R.; Zhao, N.; Osedach, T. P.; Wanger, D. D.; Chang, L.-Y.; Bawendi, M. G.; Bulovi, V. *Nano Lett.* **2011**, *11*, 2955. (c) Lin, H.; Xia, W.; Wu, H. N.; Tang, C. W. *Appl. Phys. Lett.* **2010**, *97*, 123504.